diversity

MDPI

Article

Morphological and Genetic Differentiation of *Loliolus* (*Nipponololigo*) *beka* (Cephalopoda: Loliginidae) in Coastal China

Shuwen Li [1,2], Yuhan Lyu [1,2], Chi Zhang [1] and Xiaodong Zheng [1,2,*]

[1] Key Laboratory of Mariculture, Ocean University of China, Qingdao 266003, China
[2] Institute of Evolution and Marine Biodiversity, Ocean University of China, Qingdao 266003, China
* Correspondence: xdzheng@ouc.edu.cn

Abstract: The population genetic structure of 211 samples of *Loliolus* (*Nipponololigo*) *beka*, which were selected from across seven geographic localities—in the Bohai Sea, the Yellow Sea and the East China Sea—were analyzed using mitochondrial COI and 16S rRNA gene markers. Phylogenetic trees and a haplotype network both showed that the *L.* (*N.*) *beka* localities were genetically distinct, forming two homogeneous lineages: Lineage A and Lineage B. The results of an AMOVA showed that the genetic variation in the *L.* (*N.*) *beka* populations was dominated by the genetic variation between the two lineages, and both the genetic distance and genetic differentiation indices indicated that the genetic differentiation between the two lineages of *L.* (*N.*) *beka* in Chinese waters had reached the level of species divergence. To further confirm the differences between the two lineages shown in the molecular results, we performed a detailed analysis based on morphometric observations and a multivariate statistical analysis to compare the morphology characteristics of Lineage A and Lineage B. The results showed that there were significant differences ($p < 0.05$) in the ventral mantle length (VML); the mantle width index (MWI); the fin width index (FWI); the head length index (HLI); the left Arm IV length index (LALI4), the right Arm III length index (RALI3), the right Arm IV length index (RALI4), and the hectocotylized proportion of the left Arm IV length (HcL%) between the two lineages. The differences between the two lineages were also supported by the analysis results for the number of sucker ring teeth. Accordingly, the results of the morphological analysis further confirmed the molecular analysis and provided additional evidence for the presence of the cryptic species of *L.* (*N.*) *beka* in the coastal areas of China.

Keywords: population variations; morphological diversity; cytochrome c oxidase I; 16S rRNA; cryptic species

Citation: Li, S.; Lyu, Y.; Zhang, C.; Zheng, X. Morphological and Genetic Differentiation of *Loliolus* (*Nipponololigo*) *beka* (Cephalopoda: Loliginidae) in Coastal China. *Diversity* **2023**, *15*, 41. https://doi.org/10.3390/d15010041

Academic Editor: Bert W. Hoeksema

Received: 27 October 2022
Revised: 3 December 2022
Accepted: 24 December 2022
Published: 29 December 2022

1. Introduction

Cephalopods are appealing to researchers due to their extraordinary brains and miraculous mimetic abilities. In addition, they are also an important fishery resource as they are popular among consumers all over the world because of their high protein content and good taste. They also have unique life history characteristics, such as a short lifespan; high natural mortality and turnover rates; rapid and, often, non-asymptotic growth; and diversified habitats. These characteristics mean that they can adapt quickly to environmental changes, thereby giving them a competitive advantage over other biological populations as they can fill the niche left by them in the wake of environmental changes. This results in relatively complex populations [1–3]. Furthermore, cephalopods show a wide variety of morphologies due to their wide distribution. In recent years, many hidden species of Cephalopoda have been found, such as *Uroteuthis duvaucelii* [4], *Amphioctopus neglectus* [5], and *Octopus minor* [6].

Loliolus (*Nipponololigo*) *beka* belongs to the class Cephalopoda, and is of the Myopsida order and of the Loliginidae family. It is mainly distributed across temperate to tropical environments, such as the western Pacific Ocean, and all along the south-east Asian coastal

waters—from southern Japan and Hainan Island, to the Gulf of Thailand and the Andaman Sea [7]. Its distribution across Chinese waters ranges over a wide area, which covers the Bohai Sea, the Yellow Sea, the East China Sea, and the South China Sea [8]. *L.* (*N.*) *beka* is a type of small squid with a poor swimming ability, which mainly lives offshore [8]. To date, studies on *L.* (*N.*) *beka* have mainly focused on its life history [9], classification characteristics [10,11], phylogenetic relationship [12], and nutritional composition [13]. Yang and Tan (2000) conducted a preliminary analysis of the feeding habits of *L.* (*N.*) *beka* in the Bohai Sea and showed that they are a benthic species [9]. Yang et al. (2012) conducted a comparative analysis on the morphological characteristics of the beak of the *L.* (*N.*) *beka* in the East China Sea using geometric measurements. They found that some of the characteristics were stable and did not change with the growth of the individuals [10]. *L.* (*N.*) *beka* is a widely distributed species, and the large habitat variation of the squids makes them likely to have a complex genetic structure. However, very few relevant studies on *L.* (*N.*) *beka's* population genetics and phylogeography have been reported; therefore, the population genetic variation and genetic structure of this species in Chinese waters has yet to be studied.

In the study of population differentiation, the traditional method is the most intuitive approach. This approach is mainly based on meticulous and methodical descriptions of the morphology, color patterns, and other such characteristics. In the past decades, modern taxonomy has benefited much from the progress of molecular technology and tools [14,15]. Mitochondrial DNA—with features such as a maternal inheritance, rapid evolution rate, and the negligible chances of recombination—have played a paramount role in the population genetics studies of aquatic creatures such as *Coilia nasus* [16], *Acanthopagrus schlegelii* [17], and *Johnius grypotus* [18]. Cytochrome c oxidase I (COI) and 16S rRNA (16S), in particular, have been used in species identification [19,20]. Dai et al. (2012) analyzed the possible existence of hidden species of *L.* (*N.*) *beka* in the coastal waters of China [21]. Xu et al. (2019) suggested the existence of a cryptic species of *L.* (*N.*) *beka* in China waters by analyzing the COI data of *L.* (*N.*) *beka* in Qingdao, Shandong [22]. In this study, in order to address the above questions about the differentiation of *L.* (*N.*) *beka*, we conducted molecular and morphological analyses of *L.* (*N.*) *beka.* The samples were taken from seven geographic localities along the Chinese coast to further investigate their genetic structure.

2. Materials and Methods

2.1. Sample Collection and Laboratory Procedures

L. (*N.*) *beka* was sampled from 7 regions along the Chinese coast, including Dalian (DL), Liaoning; Yantai (YT), Shandong; Qingdao (QD), Shandong; Lianyungang (LYG), Jiangsu; Nantong (NT), Jiangsu; Wenzhou (WZ), Zhejiang and Ningde (ND), Fujian (Table S1; Figure 1). These samples, collected from offshore fishing boats, are common species in the local areas; therefore, this study did not involve any endangered or protected species.

The squid samples were moved to the laboratory using cold-chain transport. A small piece of mantle muscle tissue was obtained from each individual squid and was preserved in 100% alcohol until the DNA extraction. Sucker ring samples were removed with tweezers under a stereoptometry microscope with a camera system (model: Nikon SMZ 800N, Japan), and then photographed and recorded. The samples for the morphology analysis were then fixed in a 10% formalin solution and transferred to 75% alcohol one week later for long-term storage [23] and standardized measurements.

2.2. DNA Extraction, PCR Amplification and Sequencing

The total DNA was extracted by the CTAB method, as modified by Winnepenninckx et al. (1993) [24]. The COI and 16S fragments for the population analysis were amplified through the use of the primers LCO1490/HCO2198 [25] and 16S rRNA-F/16S rRNA-R [26], in a total volume of 25 µl—which contained 9.5 µl of sterile distilled H2O; a 1 µl template DNA (approximately 100 ng); 1 µl of each primer (10 µM); and 12.5 µl 2 × Taq Master Mix (Vazyme, Nanjing, China). A PCR was run under the following cycle conditions:

pre-denaturing at 95 °C for 3 min. This was followed by 32 cycles of denaturing at 95 °C, for 15 s; annealing at 60 °C (COI) or 56 °C (16S) for 20 s; extending at 72 °C for 1 min; and then extending at 72 °C for 5 min. The PCR products were checked in 1.5% agarose gel and then sequenced using forward PCR primers on an ABI 3730xl, purchased from Sangon Biotech Company (Shanghai, China).

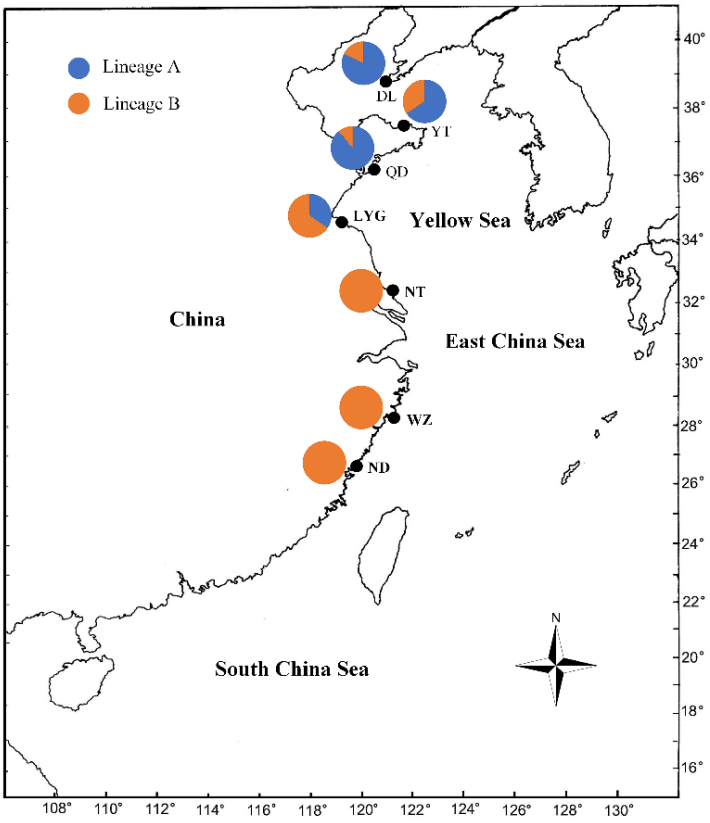

Figure 1. The sampling sites of *L.* (*N.*) *beka* and the distribution frequencies of Lineage A and Lineage B of mitochondrial DNA-based results (see below) in 7 localities. (Note: DL: Dalian; YT: Yantai; QD: Qingdao; LYG: Lianyungang; NT: Nantong; WZ: Wenzhou; and ND: Ningde. The blue in the pie chart represents Lineage A, and the orange represents Lineage B).

2.3. Sequence Data Analysis

All the sequences were aligned in SeqMan v.7.2 [27], multiplexed using Clustal W [28], and then verified separately in GenBank. MEGA v.11 [29] was used to calculate the average base composition and number of variant sites (S) for all sequences. Genetic diversity indices were calculated using DnaSP v5.10 [30], and the genetic differentiation index (F_{st}) was further evaluated using Arlequin 3.11 [31], to ascertain the level of genetic differentiation among the localities. Haplotype network maps were constructed by the median linkage method, using Popart v.1.7 [32], and then visualized and manually adjusted. Genetic distances were then calculated using MEGA v.11 [29]. Based on the haplotype network map results, an analysis of molecular variance (AMOVA) was performed using the Kimura 2-parameter model, by Arlequin 3.11, to assess the reliability of the grouping and the main drivers of genetic variation in the population [31].

Phylogenetic trees were constructed using the Bayesian inference (BI) and maximum likelihood (ML) methods, using IQ-TREE v1.6.12 [33] and MrBayes v.3.2 [34], respectively, with *Uroteuthis duvaucelii* as an outgroup. The best nucleotide substitution models were calculated using ModelFinder [35]—under the BIC (Bayesian information criteria) criterion (Table S2)—and the phylogenetic trees were further edited and visualized using FigTree v1.4.3 (http://tree.bio.ed.ac.uk/software/figtree, accessed on 23 January 2022)).

Based on the results of the phylogenetic analysis, neutrality tests (i.e., Tajima's *D* test [36] and Fu's *F*s test [37]) were calculated for each locality and the two lineages of *L.* (*N.*) *beka,* using the Arlequin 3.11 [31] software. The mismatch distribution for all the localities and lineages was constructed using DnaSP v5.10 [30], to infer the historical population dynamics.

2.4. Morphology Data Analysis

The results of the molecular experiments divided all the *L.* (*N.*) *beka* samples into two lineages: Lineage A and Lineage B. Consequently, we selected fifteen morphologically well-preserved individuals from each lineage and carried out morphological analyses on them. Fifteen morphometric characteristics and eight meristic characteristics (e.g., the number of sucker ring teeth on the largest arm sucker ring on each arm of both male and female squids) were recorded (Table S3). Male and female individuals were analyzed separately due to the differences in the hectocotylized arm (Tables S4 and S5). Most characteristics were analyzed in proportion to the dorsal mantle length (DML) to avoid the effect of size differences between the samples (Table S3) [23,38]. SPSS 26.0 was then used for an independent *t*-test and principal component analysis ($p < 0.05$).

Based on the 15 morphological indicators of the two lineages, the uncorrelated principal components that dominated the group differences were calculated. The contribution rate of the principal components and cumulative contribution were calculated according to the method of Brzeski et al. (1988) [39]. The morphological indicators were similarly analyzed using the stepwise discriminant method, and the discriminant function was constructed based on the discriminant parameters. The formula for the discriminant accuracy was calculated with reference to Gao et al. (2019) [40].

3. Results

3.1. Population Genetic Analysis, Based on Mitochondrial DNA Markers

3.1.1. Genetic Diversity of *L.* (*N.*) *beka*

In this study, 201 partial COI sequences and 192 partial 16S sequences were obtained from the squid samples. Of the 646 bp aligned for COI, 76 were variable, accounting for 11.8% of the total sequence, and 53 were parsimony-informative. The average percentages of T, C, A, and G were 35.8%, 18.8%, 29.3%, and 16.2%, respectively. With an aligned length of 478 bp in the 16S, 59 individuals were variable (accounting for 12.3% of the total length), and 35 were parsimony-informative. The average percentages of T, C, A, and G were 33.0%, 19.1%, 38.0%, and 9.9%, respectively, and the content of A + T was much higher than that of G + C, indicating an obvious AT bias.

The average values of the haplotype diversity (Hd) and nucleotide diversity (π) for all the *L.* (*N.*) *beka* populations were high overall (i.e., COI: 0.866 and 0.0310; 16S: 0.623 and 0.0214). In terms of a single locality, the diversity of the localities from DL, YT, QD, and LYG were relatively high for both COI and 16S, while the ND locality had a low value of both the Hd and π. As for the NT and WZ localities, the π values were relatively low and the Hd values differed between the COI and 16S results (Table 1).

Table 1. The genetic diversity indices for geographic localities of *L.* (*N.*) *beka*.

Group	COI				16S			
	N	**Hap**	**Hd**	π	**N**	**Hap**	**Hd**	π
DL	39	19	0.896	0.017	36	9	0.727	0.012
YT	29	16	0.916	0.029	27	5	0.553	0.017
QD	36	16	0.895	0.014	35	10	0.632	0.01
LYG	29	14	0.825	0.028	27	3	0.53	0.019
NT	14	7	0.795	0.002	14	3	0.385	0.004
WZ	28	9	0.587	0.002	28	6	0.331	0.001
ND	27	7	0.456	0.001	25	4	0.23	0.001
Total	201	64	0.866	0.031	192	20	0.623	0.021

3.1.2. Phylogenetic Relationships and Two Lineages

A total of 64 haplotypes were obtained, based on the COI sequences, of which 49 were unique haplotypes. Hap 1 and Hap 15 were the main shared haplotypes. A total of 20 haplotypes were obtained from the 16S sequence, of which four were shared haplotypes and the others were unique. Similar to the COI, 16S also had two major shared haplotypes: Hap 1 and Hap 3. Hap 1 was shared by all the localities, while Hap 3 was only shared by four localities.

The phylogenetic trees were constructed based on the 64 haplotype sequences of COI, and both the ML tree and the BI tree formed two independent branches: Lineage A and Lineage B, with the support of 1/100. The haplotype network diagram of COI also formed two independent lineages (Figure 2). For Lineage A, a total of 19 haplotypes were defined from 89 sequences, and the remaining 112 sequences belonged to Lineage B, yielding a total of 15 haplotypes. The ML and BI trees that were constructed from the 16S haplotype sequences were also identical, and both showed that the *L.* (*N.*) *beka* localities were divided into two independent clades: Lineage A and Lineage B (Figure 3). The haplotype network diagram was consistent with the phylogenetic tree results, and the evolutionary relationship was simple. The 20 haplotypes diverged into two lineages, with the star structure centered on Hap l and Hap 3, respectively.

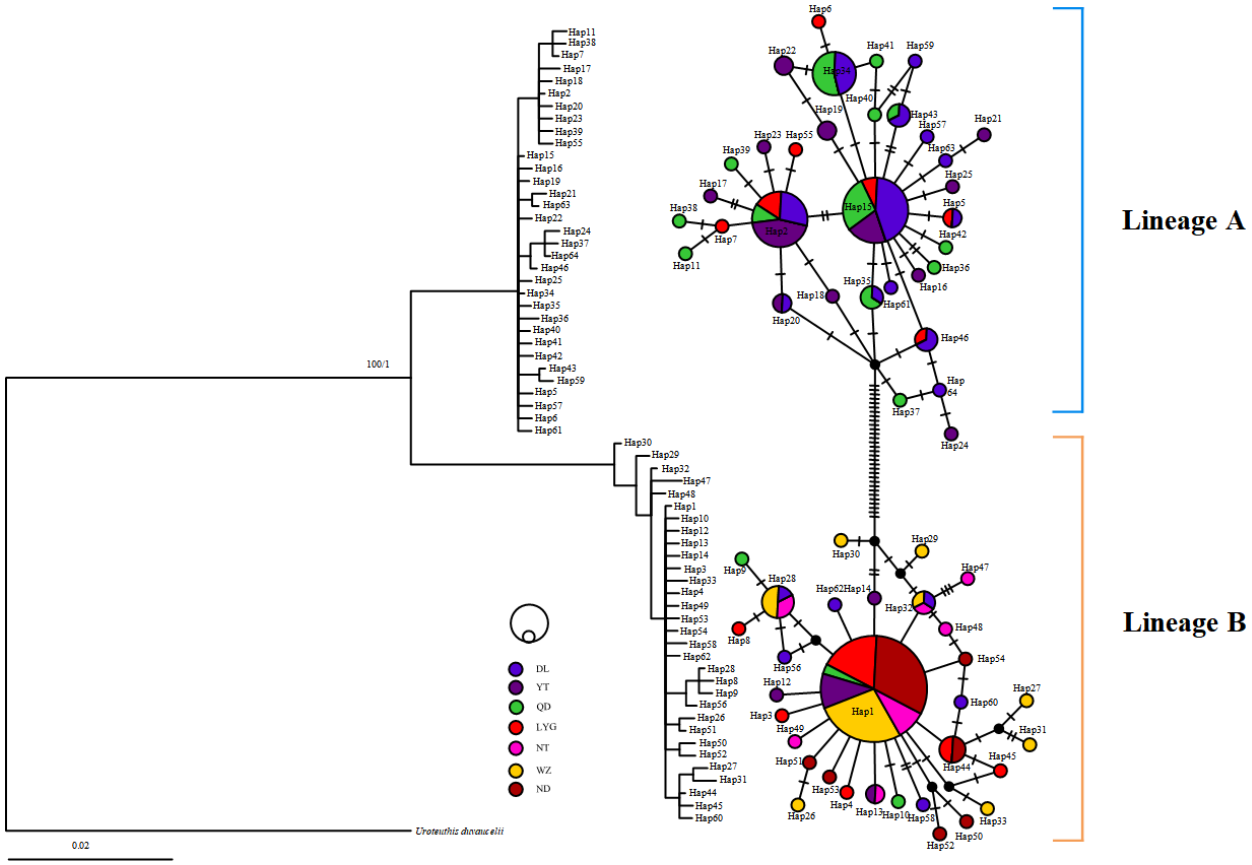

Figure 2. Maximum likelihood (ML) and Bayesian inference (BI) phylogenetic tree and haplotype network of *L.* (*N.*) *beka* based on COI haplotypes. Size of circle is proportional to the frequency of a particular haplotype. Each small line on the line that connects two circles represents a mutational step, and black dots represent hypothetical missing intermediates.

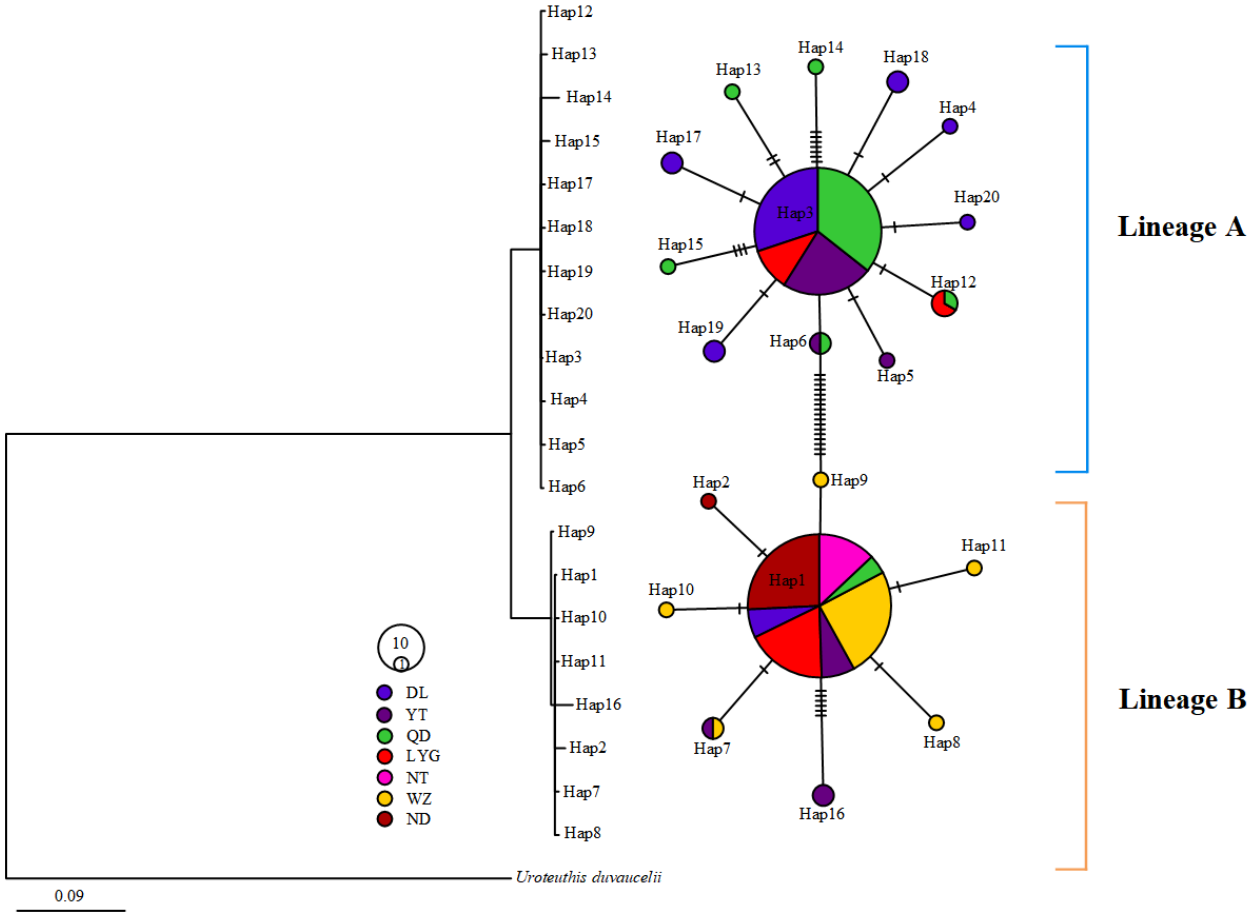

Figure 3. Maximum likelihood (ML) and Bayesian inference (BI) phylogenetic tree and haplotype network of *L.* (*N.*) *beka* based on 16S haplotypes. Size of circle is proportional to the frequency of a particular haplotype. Each small line on the line that connects two circles represents a mutational step, and black dots represent hypothetical missing intermediates.

The results of the COI and the 16S sequence analysis were consistent. Lineage A and Lineage B were sympatric and regularly distributed across DL, YT, QD, and LYG stocks, while Lineage A was only distributed across DL, YT, QD, and LYG localities, and Lineage B was distributed across all the seven localities (Figures 1–3).

3.1.3. Population Structure

The AMOVA, based on COI and 16S, divided all the seven localities into Lineage A and Lineage B. The COI result revealed a 89.78% variation among the lineages, 9.77% within populations, and 0.44% among the populations. The 16S result revealed a 96.38% variation among the lineages, 3.61% within populations, and 0.01% among the populations (Table 2). The F_{st} among the different geographical localities was −0.015 (QD vs. DL) to 0.838 (QD vs. ND) for COI, and −0.015 (QD vs. DL) to 0.841 (QD vs. WZ) for 16S. The F_{st} between the Lineages A and B was 0.900 for COI and 0.52 for 16S ($p < 0.05$), and both results indicated that there was significant genetic differentiation between Lineage A and Lineage B in *L.* (*N.*) *beka* localities (Table 3, Table S6).

According to the above analysis results, the genetic distance between Lineage A and Lineage B and the genetic distances within the lineages were calculated. Based on COI, the genetic distances within Lineages A and B were 1.0% and 0.2%, respectively, and the genetic distance between Lineage A and Lineage B was 5.9%. Based on 16S, the genetic distances within both lineages were 0.1%, while the genetic distance between both lineages was 4.2% (Table S6). The results of both the COI and 16S showed that the genetic distance between Lineage A and Lineage B was significant.

Table 2. AMOVA analysis of *L.* (*N.*) *beka* localities, based on COI and 16S.

	Source of Variation	df	Sum of Squares	Variance Component	Percentage of Variation/(%)	F Statistic
			Gene pool (Lineage A; Lineage B)			
COI	Among groups	1	1137.067	17.04307 Va	89.78	FSC: 0.04352
	Among populations	3	11.951	0.08438 Vb	0.44	FST: 0.90230
	Within populations	128	237.394	1.85464 Vc	9.77	FCT: 0.89785
	Total	132	1386.412	18.98209		
			Gene pool (Lineage A; Lineage B)			
16S rRNA	Among groups	1	518.089	9.86162 Va	96.38	FSC: 0.00324
	Among populations	2	0.801	0.00120 Vb	0.01	FST: 0.96392
	Within populations	101	37.284	0.36915 Vc	3.61	FCT: 0.96380
	Total	104	556.174	10.23197		

Table 3. *F_{st} between populations of* L. (N.) beka, *based on COI (below diagonal) and 16S (above diagonal).*

Group	DL	YT	QD	LYG	NT	WZ	ND
DL		0.017	−0.015	0.344 *	0.735 *	0.791 *	0.785 *
YT	0.067 *		0.065 *	0.166 *	0.597 *	0.681 *	0.671 *
QD	−0.015	0.111 *		0.417	0.791*	0.841 *	0.836 *
LYG	0.386 *	0.137 *	0.442 *		0.260	0.337 *	0.327 *
NT	0.738 *	0.513 *	0.792 *	0.204		0.111	0.090
WZ	0.779 *	0.588 *	0.826 *	0.271 *	−0.012		0.000
ND	0.791 *	0.604 *	0.838 *	0.291	0.079 *	0.022 *	

* Significant at $p < 0.05$.

3.1.4. Population Demography

Tajima's *D* and Fu's *F*s statistics of both the COI and 16S were all significantly negative (Table 4), indicating a possible population expansion event for the *L.* (*N.*) *beka*. The unimodal mismatch distributions were detected in each lineage (A and B), which further demonstrated that a population expansion event had happened in the species (Figure S1). The bimodal mismatch distribution was detected in all samples—corresponding to both Lineage A and Lineage B—which showed obvious genetic differentiation in the population.

Table 4. Results of neutrality test for lineages of *L.* (*N.*) *beka* based on COI and 16S.

Lineage	COI		16S	
	Tajima's *D*	Fu's *F*s	Tajima's *D*	Fu's *F*s
Lineage A	−1.391 *	−2.208 *	−2.690 *	−5.297 *
Lineage B	−2.327 *	−16.074 *	−2.360 *	−1.925 *

* Significant at $p < 0.05$.

3.2. Morphological Analysis

3.2.1. Multi-Analysis of Morphology

For the Lineage A squids, the total length (TL) was between 97.5 and 130.5 mm; the dorsal mantle length (DML) was between 29.5 and 41.5 mm, which was approximately between 1.8 and 2.0 times the mantle width (MW); the total weight (TW) was between 0.95 and 2.19 g; the arm formula was 3 > 4 > 2 > 1; Arm IV, on the left side of each of the male squids, was specialized as the hectocotylized arm, with a pointed and protruded apparatus accounting for approximately 50% of the total arm lengths (AL). Regarding the squids of Lineage B, the TL was between 109.5 and 155.5 mm and the DML was between 32.5 and 55.1 mm, which was approximately between 1.4 and 1.6 times the MW; the TW was between 2.23 and 9.25 g; the arm formula was the same as that of Lineage A; the apparatus accounted for approximately 60% of the total length of the hectocotylized arms. There were

no significant differences in the HWI, FLI, EDI, HW/HL, RALI1, and RALI2 between the Lineage A and Lineage B squids, while significant differences were observed in the VML, MWI, FWI, HLI, LALI4, RALI3, RALI4, and HcL% ($p < 0.05$), which proved that these two lineages had both similarities and differences (Figure S2).

The principal component analysis (PCA) results showed that the four components explained over 79.646% of the total morphological variance. The first principal component had contributions from MWI, HWI, HLI, FWI, LALI1, RALI1, RALI2, RALI3, RALI4, and FW/FL loadings as the most important loadings for the explained variance, which accounted for nearly 43.153% of the total variance. The second principal component had the VMLI and FLI as the most important loadings for the explained variance, with a total contribution rate of 15.321%. The third and the fourth components were HWI/HLI (12.261%) and DML (8.910%), respectively (Table S7). Shown below is a scatter plot based on the principal components one and two (Figure 4). The formula for the discriminant accuracy was calculated as follows (X1 is DML, X2 is VMLI, X3 is MWI, X4 is RALI1 and X5 is RALI2):

$$\text{Lineage A: } Y1 = 2.819X1 + 1.069X2 + 2.955X3 - 1.13X4 + 2.195X5 - 214.989 \quad (1)$$

$$\text{Lineage B: } Y2 = 3.787X1 + 0.683X2 + 4.48X3 - 2.511X4 + 3.108X5 - 311.528 \quad (2)$$

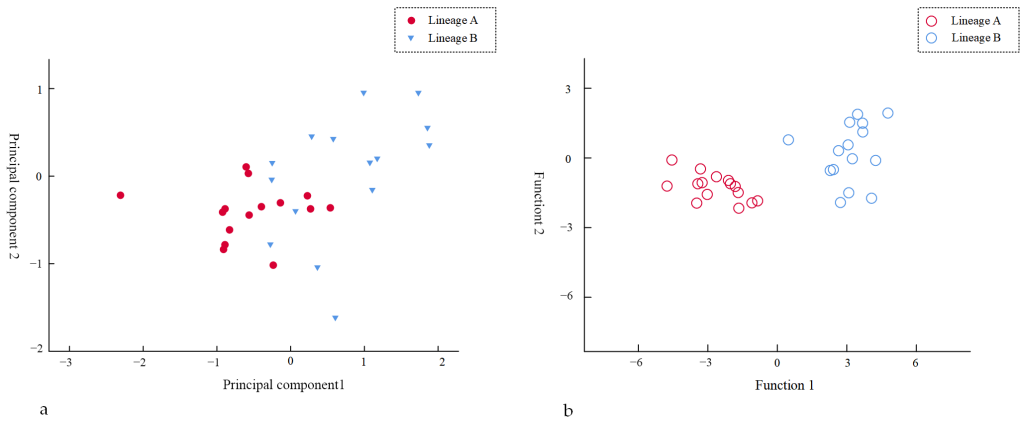

Figure 4. The scatter plot of (**a**) principal component analysis and (**b**) discriminant analysis.

The analysis showed that Lineage A and Lineage B could be clearly distinguished, with a discriminant accuracy of 100% (Table S8, Figure 4).

3.2.2. Comparison of Sucker Ring Morphology

The sucker rings from the common arms of the squids from Lineage A and Lineage B were compared. The results showed that the rings from Arm I and Arm IV of the Lineage A squids had 3–4 wide plate teeth, and that the rings from Arm II and Arm III had 4–5 wide plate teeth. The sucker rings of Arm I and Arm IV of the Lineage B squids had the same shape and number of teeth as those of Lineage A; however, the sucker rings of Arm II and Arm III had 6–8 wide plate teeth (Figure 5). Based on this, the Lineage A and Lineage B samples could be clearly distinguished through the significant differences in the sucker rings of Arm II and Arm III. We then compared the sucker rings of the Lineage A and Lineage B samples with those of the type specimen described in 1929 (Sasaki) [41]. Through this comparison, we found that the number of sucker ring teeth in the Lineage A squids was basically the same as the number described in the type specimen; however, the number of sucker ring teeth found in the squids of Lineage B differed significantly from the number described in the type specimen (Figure 6).

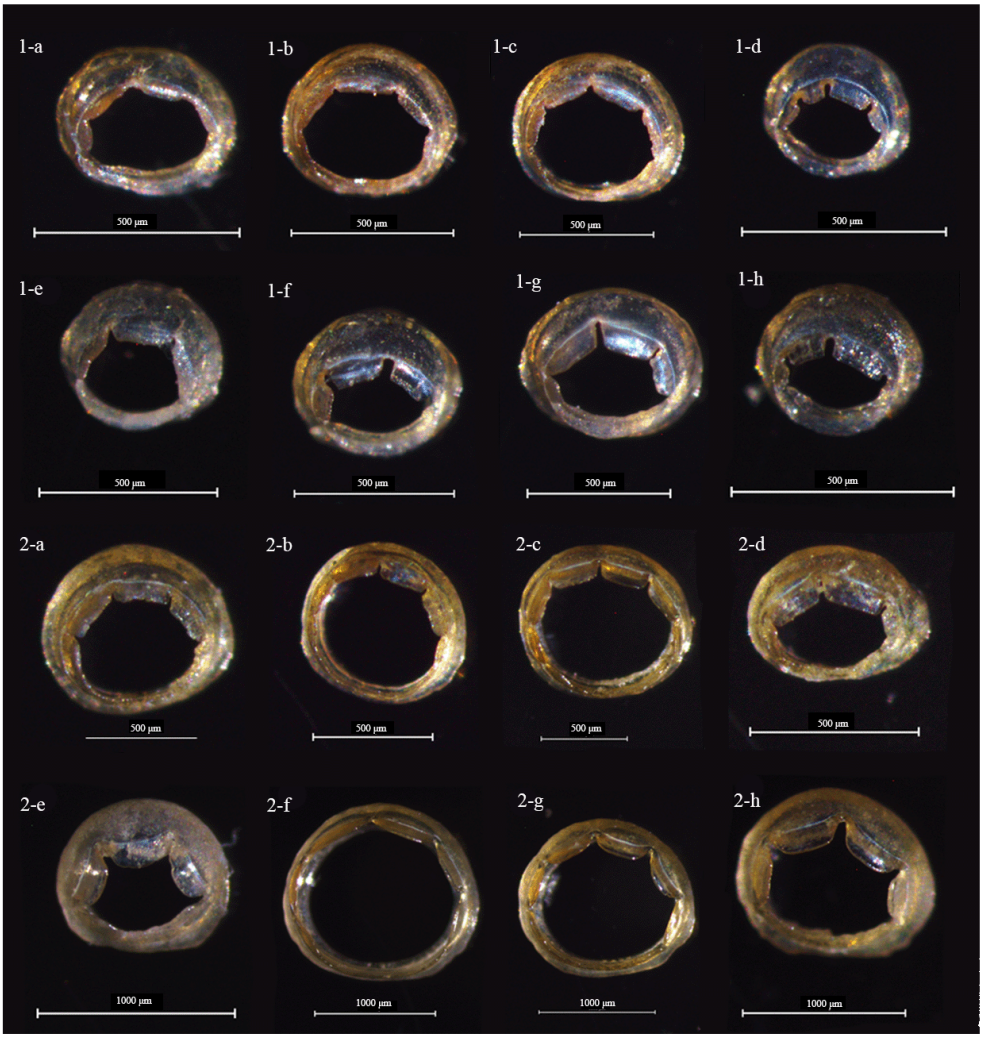

Figure 5. Sucker rings of *L.* (*N.*) *beka*. (Note: 1: Lineage A; 2: Lineage B; a: Arm I sucker ring (♀); b: Arm II sucker ring (♀); c: Arm III sucker ring (♀); d: Arm IV sucker ring (♀); e: Arm I sucker ring (♂); f: Arm II sucker ring (♂); g: Arm III sucker ring (♂); and h: Arm IV sucker ring (♂)).

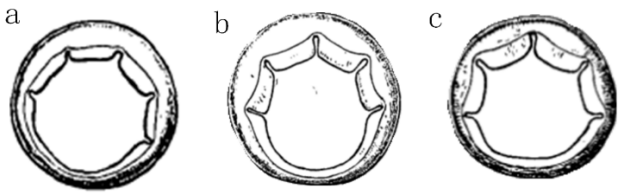

Figure 6. Sucker ring of type specimen from *L.* (*N.*) *beka* (Sasaki, 1929) 38. (**a**) proximal most sucker; (**b**) largest sucker; and (**c**) a distal sucker.

4. Discussion

4.1. Genetic Diversity of L. (N.) beka

The haplotype number (N), the haplotype diversity (Hap), and the nucleotide diversity (π) are important indicators of a population's genetic diversity, and a higher haplotype diversity and nucleotide diversity indicates a higher genetic diversity in a population [42,43]. Cephalopods are recognized as a group of organisms with relatively poor genetic variation, and data from previous studies indicate that, with the exception of a few species [44], marine cephalopods show low levels of genetic variation, which usually occurs only in populations with severe declines and which are rare in any other invertebrate group [45]

However, the results of our study showed that the *L.* (*N.*) *beka* populations had high haplotype diversity and nucleotide diversity.

L. (*N.*) *beka* is a short-lived species, with a short sexual maturation cycle and long breeding seasons. Such life history characteristics may contribute to the rapid population growth of this species and the preservation of new mutations and high Hd values [46]. The high number of single-base variants may have contributed to the relatively high π value of the population. In this study, the *L.* (*N.*) *beka* along the Chinese coast formed two branches with a large divergence in their phylogeny, and the different branches nevertheless showed a homogeneous distribution in the same region. Such a phylogeographic pattern is generally formed by the re-mixing of historically heterogeneously-divergent taxa, which, although living in the same area after mixing, have led to reproductive isolation between lineages due to long-term disruptions in the gene exchange [47]. Interestingly, we found that squids from Lineage A only occurred in northern China, and speculate that the cause of this phenomenon may be the salinity and temperature of the seawater. The temperature and salinity of the northern Chinese waters are relatively low, and the two lineages have long been distributed in waters with widely different geographical spans and environmental differences, while the long-term selective effect of marine environmental factors may also be an important factor in the north–south divergence of *L.* (*N.*) *beka* in China. In previous studies on cephalopods, Chen et al. screened genes related to osmoregulation in the adaptive differentiation of *Amphioctopus fangsiao* in different Chinese seas [45], and Du et al. suggested that the main influencing factor for the adaptive differentiation of *Octopus minor* in different Chinese seas was the salinity of the water column [46]. Therefore, we speculate that the differentiation of *L.* (*N.*) *beka* in the different Chinese waters in this study is similarly related to the large span of temperature and salinity differences along the Chinese coast.

4.2. Genetic Differentiation and Historical Dynamics

The results of the phylogenetic analysis and the haplotype network analysis indicated that there were two significantly genetically-differentiated lineages in the *L.* (*N.*) *beka* localities. The AMOVA analysis showed that the genetic variation in the *L.* (*N.*) *beka* locality mainly existed between the lineages (i.e., COI: 5.9%; 16S: 4.2%) (Table S6). Tang et al. (2010) [48] suggested that the different lineages of the sympatric distribution belonged to the different species. In this study, Lineage A was distributed and dominated only in DL, YT, QD, and LYG; however, Lineage B was distributed across all the sampling sites, but only dominated in the following four groups: LYG, NT, WZ, and ND. These two lineages were distributed homogeneously in DL, YT, QD, and LYG. This distribution is similar to the genealogical distribution of the cryptic species of the *Eriocheir sensu* (Xu et al., 2009) [49], *Cyclina sinensis* (Ni et al., 2012) [50], and *Reticunassa festiva* (Yang et al., 2020) [16]. Taken together, the genetic evidence suggests that the genetic relationship between Lineages A and B has reached the level of species differentiation; however, this needs to be further supported by the results of the morphological analysis.

In recent years, several studies have shown that, during the Pleistocene period, climate change was dramatic and had a drastic effect on the distribution and genetic structure of most marine organisms [51–53]. Considering the geographical isolation between marginal seas, the aforementioned climate change must be the main factor in the genetic differentiation in the *L.* (*N.*) *beka* populations. During the Pleistocene period, the sea level dropped and the area of each sea shrank, and both the Bohai and East China Seas were isolated, with less genetic exchange with other seas [54,55]. Thus, in turn, this led to the random divergence of *L.* (*N.*) *beka*. Glacial melt—the propulsive effect of the seawater and currents following the rise in the sea levels—caused the Lineage A and Lineage B populations to rapidly expand and to occupy new ecological niches [56]. This finding has been supported by mismatch distribution maps and neutrality tests. The divergent lineages, which were generated by the aforementioned geographic isolation during this age, came into contact with each other twice during the late Pleistocene population expansion and, thus, formed a suture zone [50,53,57]. In contrast to the *Mugil cephalus* lineage, which only made secondary

contact between relatively close sea area intervals and for which the genetic differences between the two sides of the suture zone were significant, the suture zone of the *L.* (*N.*) *beka* lineage ran through all the sampling sites of Lineage A. We speculate that this phenomenon may be due to the wide range of temperature and salinity adaptations in the ancestral locality of Lineage B [58], which may have resulted in the present distribution pattern. Whether there is hybridization or gene mixing between Lineage A and Lineage B needs to be verified by a subsequent analysis of the nuclear genes among the localities. In addition, previous studies have also shown that geohistorical events and currents are important factors, which have influenced the differentiation of cephalopods in China [59]. In the present study, the population history dynamics test indicated that the *L.* (*N.*) *beka* taxa have experienced population expansion in history; however, determining whether geohistorical events and ocean currents are the causes of the divergence between the two lineages will require a further in-depth study.

4.3. Morphological Variation among Localities

In this study, the morphological characteristics of Lineage A and Lineage B were compared using 15 morphological parameters. The results showed that there were characteristics that did not differ between the two lineages, which indicates the homology of the morphological characteristics of *L.* (*N.*) *beka;* however, the results also showed that there were characteristics with significant differences, which could be used to differentiate between the two lineages. Both a principal component analysis and a discriminant analysis were able to effectively distinguish the squids of Lineage A from those of Lineage B (Figure 4). It is noteworthy that the hectocotylized arms of the male squids are specialized and found on the fourth arm on the left side. These arms have the function of transmitting spermatophore during mating. The morphology and length of the hectocotylized arms of the different species were found to be significantly different, which is an important morphological trait that can be used to distinguish between the different species of squids [5,60]. The hectocotylized proportion of the Lineage B samples accounted for a larger proportion of the hectocotylized arms, approximately 58%, while the Lineage A samples accounted for approximately 50%.

Moreover, the numbers and shape of the sucker ring teeth were stable in mature individuals, and this characteristic varied significantly among the species, which is an important basis for the taxonomic discrimination of squids 5. In this study, the numbers of sucker ring teeth in the squids from Lineage A (4–5) and Lineage B (6–8) were significantly different, which could be used as a strong indicator to distinguish individuals from these two lineages.

Thus, we compared the morphometric indices and sucker rings of Lineage A and Lineage B squid samples with the type specimens of *L.* (*N.*) *beka* described by Sasaki (1929) (Table 5, Figure 6) [41]. It was found that most of the characteristics that were described for the Lineage A samples were the same or similar to those of Sasaki's type specimens, while differences in other indices (such as HcL%) may be due to incomplete data coverage with the type specimens; however, for Lineage B, only LALI4, FWI, RALI1, and RALI2 showed any similarity to the description of the type specimens (Table 5, Figure 6). Such results suggest that the Lineage A individuals of *L.* (*N.*) *beka* were consistent with the type specimens originally described by Sasaki, while the Lineage B *L.* (*N.*) *beka* differed significantly from them. Therefore, we have assumed that the squids of Lineage B are a cryptic species of *L.* (*N.*) *beka* in coastal China, due to the apparent differences in the number of sucker ring teeth and the HcL%.

Table 5. Comparison of morphological measurements of *L.* (*N.*) *beka* Lineage A and Lineage B with type specimens.

	Lineage A ♀			**Lineage A ♂**			**Lineage B ♀**			**Lineage B ♂**			**L. (N.) beka ***	
	Mean	**SD**	**Range**	**Mean**	**SD**	**Range**	**Mean**	**SD**	**Range**	**Mean**	**SD**	**Range**	♀	♂
DML/mm	37.8	3.5	33.5–41.5	33.3	2.3	29.5–36.5	42.4	8.0	32.5–55.1	38.5	3.9	31.5–42.8	67.0	53.0
VMLI	84.9	3.4	80.7–89.0	87.5	3.9	81.4–94.5	81.0	5.3	69.9–85.5	83.9	6.1	78.3–93.6	83.6	83.0
MWI	43.8	3.0	39.8–46.8	47.5	4.5	42.0–57.4	59.6	4.8	52.2–66.2	59.4	4.3	50.9–65.1	29.9	34.0
HWI	40.2	7.9	30.1–49.3	46.4	5.3	40.3–57.4	46.0	4.1	40.1–52.1	51.1	3.5	45.9–55.3	23.9	28.3
HLI	32.1	3.6	29.1–37.3	34.7	3.4	30.0–39.7	36.4	2.0	33.6–38.5	38.7	3.9	33.3–42.8	23.9	32.1
FLI	55.4	2.6	53.0–58.2	55.5	3.8	49.3–60.7	55.3	3.2	49.3–59.6	56.8	1.6	53.2–58.7	59.7	66.0
FWI	56.0	6.4	49.3–64.6	62.6	5.3	54.9–70.5	70.2	3.3	66.3–74.6	71.5	5.8	65.9–81.5	61.2	66.0
LALI4	52.9	3.9	49.4–58.2	51.7	4.4	42.5–57.8	57.0	5.0	51.8–67.7	74.6	10.1	63.9–94.8	52.2	56.6
RALI1	34.1	2.8	31.5–38.0	34.4	4.0	29.6–41.0	29.3	3.4	25.1–35.4	38.6	2.3	36.1–42.5	37.3	49.1
RALI2	50.8	7.9	39.8–58.2	50.4	6.2	43.3–63.1	46.6	5.1	41.5–55.6	65.5	7.3	55.5–76.6	52.2	66.0
RALI3	60.0	5.9	51.8–64.4	64.5	5.6	56.2–74.6	67.1	6.6	58.4–77.8	81.4	3.8	74.6–87.0	59.7	69.8
RALI4	39.8	26.6	50.7–55.2	52.0	3.5	45.2–57.1	57.8	3.2	54.9–64.2	70.3	6.7	60.3–79.2	52.2	60.4
HW/HL	1.3	0.2	1.0–1.4	1.3	0.1	1.1–1.5	1.3	0.1	1.2–1.4	1.3	0.2	1.1–1.5	1.0	0.9
FW/FL	1.0	0.1	0.9–1.1	1.1	0.1	1.0–1.2	1.3	0.1	1.1–1.5	1.3	0.1	1.1–1.4	1.0	1.0
HL%	/	/	/	50	0.0	43.3–61.3	/	/	/	60	0.0	52.3–65.1	/	66.0

* Type specimens of *L.* (*N.*) *beka* described by Sasaki (1929) 41.

Combined with the molecular data, these morphological data further indicate the possible existence of a cryptic species of *L.* (*N.*) *beka* in coastal China; however, to accurately discern the relationship between the two lineages of *L.* (*N.*) *beka* by morphology, more samples need to be measured, using more morphological features, especially the internal anatomical features, which were not measured in this paper. Further studies are also needed to distinguish the factors that drive the variation in the morphological indices of *L.* (*N.*) *beka*, among the different geographic groups.

5. Conclusions

In this study, we collected 211 squid samples, from seven natural localities of *L.* (*N.*) *beka*. We analyzed their genetic diversity and genetic structure, based on their mitochondrial DNA sequences and morphological data. A multivariate analysis of 15 morphological characteristics revealed that there were two different types of *L.* (*N.*) *beka* off the coast of China, with significant differences in the morphological data of VML, MWI, FWI, HLI, LALI4, RALI3, RALI4, and HcL%. This result was also supported by the number of sucker ring teeth on the arms of the squids from each lineage. Meanwhile, a molecular data analysis, which was based on the mitochondrial genes COI and 16S, classified the *L.* (*N.*) *beka* into two lineages, between which the genetic distances (i.e., COI: 5.9%; 16S: 4.2%) and genetic differentiation indices (i.e., COI: 0.900; 16S: 0.952) reached the level of species differentiation. This indicates the existence of a cryptic species of *L.* (*N.*) *beka* in Chinese waters. This study has provided a theoretical reference for the study of species diversification and the reasonable exploitation of *L.* (*N.*) *beka* fishery resources in China.

Supplementary Materials: The following supporting information can be downloaded at: https://www.mdpi.com/article/10.3390/d15010041/s1, Table S1: Sample collection information of seven geographical localities of *L.* (*N.*) *beka*; Table S2: The optimal nucleotide substitution model of *L.* (*N.*) *beka* COI and 16S; Table S3: Morphological characters recorded on *L.* (*N.*) *beka*; Table S4: Standardized data of *L.* (*N.*) *beka* Lineage A for morphological characteristics analyses (D: damaged); Table S5: Standardized data of *L.* (*N.*) *beka* Lineage B for morphological characteristics analyses (D: damaged); Table S6: Mean genetic distances within (below diagonal) and between (diagonal) lineages and F_{st} (above diagonal) of *L.* (*N.*) *beka* based on COI and 16S; Table S7: Contribution and load of principal components on morphological characteristics of *L.* (*N.*) *beka*; Table S8: Discriminant results of Lineage A and Lineage B of *L.* (*N.*) *beka*; Figure S1: Mismatch distribution based on COI and 16S of *L.* (*N.*) *beka*; Figure S2: Statistical chart of 15 body size traits of two lineages of *L.* (*N.*) *beka* (Lineage A and Lineage B).

Author Contributions: X.Z. and Y.L. designed the study; S.L. wrote the original draft; X.Z. and S.L. reviewed and edited the paper; C.Z. collected the samples; Y.L. performed the experiments and analyses. All authors have read and agreed to the published version of the manuscript.

Funding: This work was supported by the National Natural Science Foundation of China under Grant 32170536.

Institutional Review Board Statement: All experiments involving the handling and treatment of animals were conducted in strict accordance with the recommendations in the Guide for Animal Care.

Informed Consent Statement: Not applicable.

Data Availability Statement: NCBI database gene bank accessions (COI: OP894933-OP894996; 16S: OP881570-OP881589).

Acknowledgments: We thank Chung Cheng Lu for his valuable suggestions during the planning and course of the study. The authors thank Jianzhong Guo, Zhaoyang Liu for sample collection and Jian Zheng for his helpful guidance during the article writing.

Conflicts of Interest: The authors declare no conflict of interest.

References

1. Clarke, M.R. Cephalopods as prey. III Cetaceans. *Philos. Trans. R. Soc. Lond. B Biol. Sci.* **1996**, *351*, 1053–1065.
2. Arkhipkin, A.I.; Hendrickson, L.C.; Payá, I.; Pierce, G.J.; Roa-Ureta, R.H.; Robin, J.-P.; Winter, A. Stock assessment and management of cephalopods: Advances and challenges for short-lived fishery resources. *ICES J. Mar. Sci.* **2020**, *78*, 714–730. [CrossRef]
3. Doubleday, Z.A.; Prowse, T.A.; Arkhipkin, A.; Pierce, G.J.; Semmens, J.; Steer, M.; Leporati, S.C.; Lourenço, S.; Quetglas, A.; Sauer, W.; et al. Global proliferation of cephalopods. *Curr. Biol.* **2016**, *26*, R406–R407. [CrossRef] [PubMed]
4. Lv, Y.H.; Zhang, C.; Dai, L.N.; He, W.T.; Zheng, X.D. Morphological variation analysis of *Uroteuthis Duvaucelii* in the coastal waters of Western Pacific. *Oceanol. Limnol. Sin.* **2022**, *53*, 768–777.
5. Tang, Y.; Zheng, X.; Liu, H.; Sunxie, F. Population genetics and comparative mitogenomic analyses reveal cryptic diversity of *Amphioctopus neglectus* (Cephalopoda: Octopodidae). *Genomics* **2020**, *112*, 3893–3902. [CrossRef]
6. Xu, R.; Bo, Q.; Zheng, X. A divergent lineage among *Octopus minor* (Sasaki, 1920) populations in the Northwest Pacific supported by DNA barcoding. *Mar. Biol. Res.* **2018**, *14*, 335–344. [CrossRef]
7. Jereb, P.; Vecchione, M.; Roper, C.F.E. Family Loliginidae. In *Cephalopods of the World. An Annotated and Illustrated Catalogue of Species Known to Date. Volume 2. Myopsid and Oegopsid Squids*; Jereb, P., Roper, C.F.E., Eds.; FAO Species Catalogue for Fishery Purposes; FAO: Rome, Italy, 2010; Volume 2, pp. 38–117.
8. Dong, Z.Z. *Fauna Sinica. Phylum Mollusca. Class Cephalopoda*; Science Press: Beijing, China, 1988; pp. 181–182.
9. Yang, J.M.; Tan, X. Food Analysis of three cephalopod species in the Bohai Sea. *Mar. Sci.* **2000**, *244*, 53–55.
10. Yang, L.L.; Jiang, Y.Z.; Liu, Z.L.; Lin, N.; Li, S.F.; Cheng, J.H. Analysis of beak morphology of *Loligo beka* in the East China Sea. *J. Fish. Sci. China* **2012**, *19*, 586–593. [CrossRef]
11. Jin, Y.; Liu, B.; Li, J.; Chen, X. Identification of three common Loliginidae squid species in the South China Sea by analyzing hard tissues with geometric outline method. *J. Ocean Univ. China* **2017**, *16*, 840–846. [CrossRef]
12. Kang, L.; Zhang, S.; Wu, C.; Liu, X.; Xu, M.Y.; Jiang, L. Molecular phylogeny of Loliginidae inferred from mitochondrial DNA sequence variation. *Mitochondrial DNA Part A* **2017**, *29*, 600–605. [CrossRef]
13. Zheng, X.D.; Zhu, J.Y. Determination and Analysis of Cholesterol and Taurine in 4 Kinds of Different Tissues of 5 Cephalopods. *J. Oceanol. Limnol.* **2018**, *2*, 125–130.
14. Radulovici, A.E.; Archambault, P.; Dufresne, F. DNA Barcodes for Marine Biodiversity: Moving Fast Forward? *Diversity* **2010**, *2*, 450–472. [CrossRef]
15. Sanchez, G.; Setiamarga, D.H.; Tuanapaya, S.; Tongtherm, K.; Winkelmann, I.E.; Schmidbaur, H.; Umino, T.; Albertin, C.; Allcock, L.; Perales-Raya, C.; et al. Genus-level phylogeny of cephalopods using molecular markers: Current status and problematic areas. *Peerj* **2018**, *6*, e4331. [CrossRef]
16. Gao, T.; Ying, Y.; Yang, Q.; Song, N.; Xiao, Y. The Mitochondrial Markers Provide New Insights into the Population Demographic History of *Coilia nasus* With Two Ecotypes (Anadromous and Freshwater). *Front. Mar. Sci.* **2020**, *7*, 576161. [CrossRef]
17. Zhao, L.; Shan, B.; Song, N.; Gao, T. Genetic diversity and population structure of *Acanthopagrus schlegelii* inferred from mtDNA sequences. *Reg. Stud. Mar. Sci.* **2020**, *41*, 101532. [CrossRef]
18. Zhao, L.; Yi, D.; Li, C.; Sun, D.; Xu, H.; Gao, T. Phylogeography and population structure of *Johnius grypotus* (Richardson, 1846) as revealed by mitochondrial control region sequences. *ZooKeys* **2017**, *705*, 143. [CrossRef]
19. Bolstad, K.S.; Braid, H.E.; Strugnell, J.M.; Lindgren, A.R.; Lischka, A.; Kubodera, T.; Laptikhovsky, V.L.; Labiaga, A.R. A mitochondrial phylogeny of the family Onychoteuthidae (Cephalopoda: Oegopsida). *Mol. Phylogenet. Evol.* **2018**, *128*, 88–97. [CrossRef] [PubMed]
20. Strugnell, J.; Norman, M.; Jackson, J.; Drummond, A.J.; Cooper, A. Molecular phylogeny of coleoid cephalopods (Mollusca: Cephalopoda) using a multigene approach; the effect of data partitioning on resolving phylogenies in a Bayesian framework. *Mol. Phylogenet. Evol.* **2005**, *37*, 426–441. [CrossRef]
21. Dai, L.; Zheng, X.; Kong, L.; Li, Q. DNA barcoding analysis of Coleoidea (Mollusca: Cephalopoda) from Chinese waters. *Mol. Ecol. Resour.* **2012**, *12*, 437–447. [CrossRef]
22. Xu, R.; Lv, Y.; Tang, Y.; Chen, Z.; Xu, C.; Zhang, X.; Zheng, X. DNA barcoding reveals a mysterious high species diversity of conifer-feeding aphids in the mountains of southwest China. *Front. Mar. Sci.* **2022**, *9*, 2296–7745.
23. Roper, C.F.E.; Voss, G.L. Guidelines for taxonomic descriptions of cephalopod species. The biology and resource potential of cephalopods. *Memoirs Natl. Mus. Vic.* **1983**, *44*, 48–63. [CrossRef]
24. Winnepenninckx, B. Extraction of high molecular weight DNA from molluscs. *Trends Genet.* **1993**, *9*, 407. [PubMed]
25. Folmer, O.; Black, M.; Hoeh, W.; Lutz, R.; Vrijenhoek, R. DNA primers for amplification of mitochondrial cytochrome c oxidase subunit I from diverse metazoan invertebrates. *Mol. Mar. Biol. Biotechnol.* **1994**, *3*, 294–299. [PubMed]
26. Guzik, M.T.; Norman, M.D.; Crozier, R.H. Molecular phylogeny of the benthic shallow-water octopuses (Cephalopoda: Octopodinae). *Mol. Phylogenet. Evol.* **2005**, *37*, 235–248. [CrossRef]
27. Swindell, S.R.; Plasterer, T.N. *Seqman. Sequence Data Analysis Guidebook*; Springer: Totowa, NJ, USA, 1997; pp. 75–89.
28. Thompson, J.D.; Higgins, D.G.; Gibson, T.J. CLUSTAL W: Improving the sensitivity of progressive multiple sequence alignment through sequence weighting, position-specific gap penalties and weight matrix choice. *Nucleic Acids Res.* **1994**, *22*, 4673–4680. [CrossRef] [PubMed]

29. Tamura, K.; Stecher, G.; Kumar, S. MEGA11: Molecular Evolutionary Genetics Analysis Version 11. *Mol. Biol. Evol.* **2021**, *38*, 3022–3027. [CrossRef] [PubMed]
30. Librado, P.; Rozas, J. DnaSP v5: A software for comprehensive analysis of DNA polymorphism data. *Bioinformatics* **2009**, *25*, 1451–1452. [CrossRef] [PubMed]
31. Excoffier, L.; Lischer, H.E.L. Arlequin suite ver 3.5: A new series of programs to perform population genetics analyses under Linux and Windows. *Mol. Ecol. Resour.* **2010**, *10*, 564–567. [CrossRef]
32. Leigh, J.W.; Bryant, D. POPART, full-feature software for haplotype network construction. *Methods Ecol. Evol.* **2015**, *6*, 1110–1116. [CrossRef]
33. Nguyen, L.-T.; Schmidt, H.A.; Von Haeseler, A.; Minh, B.Q. IQ-TREE: A Fast and Effective Stochastic Algorithm for Estimating Maximum-Likelihood Phylogenies. *Mol. Biol. Evol.* **2015**, *32*, 268–274. [CrossRef]
34. Ronquist, F.; Teslenko, M.; Van Der Mark, P.; Ayres, D.L.; Darling, A.; Höhna, S.; Larget, B.; Liu, L.; Suchard, M.A.; Huelsenbeck, J.P. MrBayes 3.2, efficient Bayesian phylogenetic inference and model choice across a large model space. *Syst. Biol.* **2012**, *61*, 539–542. [CrossRef]
35. Kalyaanamoorthy, S.; Minh, B.Q.; Wong, T.K.F.; Von Haeseler, A.; Jermiin, L.S. ModelFinder: Fast model selection for accurate phylogenetic estimates. *Nat. Methods* **2017**, *14*, 587–589. [CrossRef]
36. Tajima, F. Statistical method for testing the neutral mutation hypothesis by DNA polymorphism. *Genetics* **1989**, *123*, 585–595. [CrossRef] [PubMed]
37. Fu, Y.-X. Statistical Tests of Neutrality of Mutations Against Population Growth, Hitchhiking and Background Selection. *Genetics* **1997**, *147*, 915–925. [CrossRef] [PubMed]
38. Liao, C.H.; Liu, T.Y.; Hung, C.Y. Morphometric variation between the swordtip (*Photololigo edulis*) and mitre (*P. chinensis*) squids in the waters off Taiwan. *J. Mar. Sci. Technol.* **2010**, *18*, 405–412.
39. Brzeski, V.J.; Doyle, R.W. A Morphometric Criterion for Sex Discrimination in Tilapia. In *The Second International Symposium on Tilapia in Aquaculture, ICLARM Conference Proceeding*; Department of Fisheries: Bangkok, Thailand; International Center of Living Aquatic Resources Management: Manila, Philippines, 1988; pp. 439–444.
40. Gao, X.; Xu, R.; Zhang, Z.; Zheng, X. Morphological variation analysis of *Octopus minor* in the coastal waters of China. *J. Fish. China* **2019**, *43*, 1593–1602.
41. Sasaki, M. A monograph of the dibranchiate cephalopods of the Japanese and adjacent waters. *J. Coll. Agric. Hokkaido Univ.* **1929**, *20*, 1–357.
42. Tajima, F. Evolutionary relationship of DNA sequences in finite populations. *Genetics* **1983**, *105*, 437–460. [CrossRef] [PubMed]
43. Weir, B.S. Genetic Data Analysis. *Biometrics* **1990**, *18*, 639. [CrossRef]
44. Katugin, O.N. Intraspecific genetic variation and population differentiation of the squid *Berryteuthis magister* in the North Pacific Ocean. *Russ. J. Mar. Biol.* **1999**, *25*, 34–45.
45. Muhammad, F.; Chen, W.; Liu, L.; Gong, L.; Du, X.; Shafi, M.; Lü, Z.-M. Genetic structure of *Amphioctopus fangsiao* (Mollusca, Cephalopoda) in Chinese waters inferred from variation in three mtDNA genes (ATPase 6, ND2, and ND5). *Hydrobiologia* **2019**, *838*, 111–119. [CrossRef]
46. Muhammad, F.; Lü, Z.-M.; Liu, L.; Gong, L.; Du, X.; Shafi, M.; Kaleri, H.A. Genetic structure of *Octopus minor* around Chinese waters as indicated by nuclear DNA variations (Mollusca, Cephalopoda). *ZooKeys* **2018**, *775*, 1–14. [CrossRef] [PubMed]
47. Zheng, X.D.; Wang, R.C.; Wang, Z.P. Advances of studies on Cephalopoda genetic variation. *J. Fish. China* **2001**, *25*, 84–89.
48. Tang, W.; Lshimatsu, A.; Fu, C.; Yin, W.; Li, G.; Chen, H.; Wu, Q.; Li, B. Cryptic Species and Historical Biogeography of *Eel Gobies* (Gobioidei: Odontamblyopus) Along the Northwestern Pacific Coast. *Zool. Sci.* **2010**, *27*, 8–13. [CrossRef] [PubMed]
49. Xu, J.; Chan, T.-Y.; Tsang, L.M.; Chu, K.H. Phylogeography of the mitten crab *Eriocheir sensu stricto* in East Asia: Pleistocene isolation, population expansion and secondary contact. *Mol. Phylogenet. Evol.* **2009**, *52*, 45–56. [CrossRef] [PubMed]
50. Ni, G.; Li, Q.; Kong, L.; Zheng, X. Phylogeography of Bivalve *Cyclina sinensis*: Testing the Historical Glaciations and Changjiang River Outflow Hypotheses in Northwestern Pacific. *PLoS ONE* **2012**, *7*, e49487. [CrossRef]
51. Galloway, R.W. Late cainozoic environments in Australia. *Ecol. Biogeogr. Aust.* **1981**, 53–80. [CrossRef]
52. Wang, P. Response of Western Pacific marginal seas to glacial cycles: Paleoceanographic and sedimentological features. *Mar. Geol.* **1999**, *156*, 5–39. [CrossRef]
53. Hewitt, G.M. Speciation, hybrid zones and phylogeography—Or seeing genes in space and time. *Mol. Ecol.* **2001**, *10*, 537–549. [CrossRef]
54. Zhao, D.; Li, Q.; Kong, L.; Yu, H. Cryptic diversity of marine gastropod *Monodonta labio* (Trochidae), did the early Pleistocene glacial isolation and sea surface temperature gradient jointly drive diversification of sister species and/or subspecies in the Northwestern Pacific? *Mar. Ecol.* **2017**, *38*, e12443. [CrossRef]
55. Zhao, D.; Kong, L.; Yu, H.; Li, Q. Cryptic genetic diversity of *Neverita didyma* in the coast of China revealed by phylogeographic analysis: Implications for management and conservation. *Conserv. Genet.* **2018**, *19*, 275–282. [CrossRef]
56. Avise, J.C. Phylogeography, retrospect and prospect. *J. Biogeogr.* **2009**, *36*, 3–15. [CrossRef]
57. Nielsen, E.E.; Nielsen, P.H.; Meldrup, D.; Hansen, M.M. Genetic population structure of turbot (*Scophthalmus maximus* L.) supports the presence of multiple hybrid zones for marine fishes in the transition zone between the Baltic Sea and the North Sea. *Mol. Ecol.* **2004**, *13*, 585–595. [CrossRef] [PubMed]

58. Shen, K.-N.; Jamandre, B.W.; Hsu, C.-C.; Tzeng, W.-N.; Durand, J.-D. Plio-Pleistocene sea level and temperature fluctuations in the northwestern Pacific promoted speciation in the globally-distributed flathead mullet *Mugil cephalus*. *BMC Evol. Biol.* **2011**, *11*, 83. [CrossRef]
59. Hewitt, G.M. The genetic legacy of the Quaternary ice ages. *Nature* **2000**, *405*, 907–913. [CrossRef]
60. Brakoniecki, T.F. *A Generic Revision of the Family Loliginidae (Cephalopoda; Myopsida) Based Primarily on the Comparative Morphology of the Hectocotylus (Zoogeography)*; University of Miami: Coral Gables, FL, USA, 1986.